

Heat capacity and thermal expansion study of $\text{Ba}_{0.9}\text{Bi}_{0.067}(\text{Ti}_{1-x}\text{Zr}_x)\text{O}_3$ ceramics

This article has been downloaded from IOPscience. Please scroll down to see the full text article.

2007 J. Phys.: Condens. Matter 19 346237

(<http://iopscience.iop.org/0953-8984/19/34/346237>)

View [the table of contents for this issue](#), or go to the [journal homepage](#) for more

Download details:

IP Address: 129.252.86.83

The article was downloaded on 29/05/2010 at 04:30

Please note that [terms and conditions apply](#).

Heat capacity and thermal expansion study of $\text{Ba}_{0.9}\text{Bi}_{0.067}(\text{Ti}_{1-x}\text{Zr}_x)\text{O}_3$ ceramics

Michail Gorev¹, Vitaly Bondarev¹, Igor Flerov¹, Mario Maglione² and Annie Simon²

¹ L V Kirensky Institute of Physics, Siberian Division, Russian Academy of Sciences, Akademgorodok, Krasnoyarsk 660036, Russia

² ICMCB-CNRS, Université de Bordeaux I, 87 avenue A Schweitzer, 33608 Pessac, France

E-mail: gorev@iph.krasn.ru and maglione@icmcb-bordeaux.cnrs.fr

Received 11 May 2007

Published 1 August 2007

Online at stacks.iop.org/JPhysCM/19/346237

Abstract

For $\text{Ba}_{0.9}\text{Bi}_{0.067}(\text{Ti}_{1-x}\text{Zr}_x)\text{O}_3$ ($x = 0.04, 0.15$) ceramics, the heat capacity $C_p(T)$ and the thermal expansion $\alpha(T)$ were measured using an adiabatic calorimeter and an optical–mechanical dilatometer in the temperature range 100–420 K. Both compounds reveal diffuse heat capacity and thermal expansion anomalies: three anomalies in the temperature regions 150–250 K, 250–300 K ($\alpha(T)$ only) and 300–400 K at $x = 0.04$ and two anomalies in the regions 200–250 K and 250–350 K at $x = 0.15$. The results obtained are discussed together with the data on the dielectric properties.

1. Introduction

BaTiO_3 based solid solutions with isovalent substitution such as $\text{Ba}(\text{Ti}_{1-x}\text{Zr}_x)\text{O}_3$ have been a subject of extensive studies. These compounds are characterized by both ferroelectric and relaxor properties depending on the composition: the original ferroelectric transitions of BaTiO_3 continuously transform at $x \gtrsim 0.25$ into the relaxor state whose temperature of occurrence (T_m) decreases to very low temperatures as the Zr content increases [1–3].

The relaxor features of $\text{Ba}(\text{Ti}_{1-x}\text{Zr}_x)\text{O}_3$ are connected with their structural (compositional) inhomogeneity or disorder and with the presence of polar nanodomains in the nonpolar matrix. The nature and the mechanism of the compositional disordering and the relaxor behaviour in Ba-containing compounds are widely discussed [4–6].

It should be pointed out that Zr substitution on B sites is isovalent, and is not predicted, accordingly, to affect in a drastic way the charge state of BaTiO_3 . Zr^{4+} ions do not act as random electric field sources. However, the Zr^{4+} ion size (72 pm) is about 20% larger than that of Ti^{4+} ions (60.5 pm) in 6 coordination, and random elastic fields are thus expected from this substitution, which are very likely to be responsible for relaxor properties which appear in BTZ for $x > 0.25$.

The heterovalent substitution of Ba^{2+} cations with the Bi^{3+} ones in $\text{BaTi}_{1-x}\text{Zr}_x\text{O}_3$ compounds can allow adding further disorder on the B sites of the perovskite lattice. It has been suggested [7] that heterovalent substitutions could induce a relaxor behaviour at low concentrations of Zr (~ 0.04). The difference in valencies of Ba and Bi would be, in that case, the more relevant parameter, and the corresponding random fields are thus expected to be of electrical nature. The cation Bi^{3+} was chosen due to its $6(\text{sp})^2$ lone pair; such electronic environments are favourable for the relaxor effect.

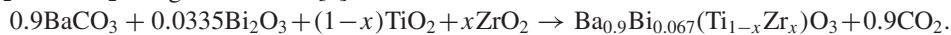
The T_c value for $\text{Ba}_{1-y}\text{Bi}_{2y/3}\text{TiO}_3$ compounds is practically stable up to the value $y = 0.10$; however the two dielectric permittivity anomalies at temperatures T_1 and T_2 merged for $y \geq 0.02$ into one at T'_m which arises within the ferroelectric state and is characterized by significant frequency dispersion [8]. Zr substitution in $\text{Ba}_{0.9}\text{Bi}_{0.067}(\text{Ti}_{1-x}\text{Zr}_x)\text{O}_3$ decreases T_c and increases T'_m up to a composition $x \approx 0.07$, beyond which there remains a single effect at T''_m with a strong dispersion, characteristic for relaxor behaviour [8].

This is very unusual in the field of relaxors where the succession of transitions is always in the thermodynamically favourable sequence on cooling: paraelectric \rightarrow relaxor \rightarrow ferroelectric. The very peculiar behaviour of $\text{Ba}_{0.9}\text{Bi}_{0.067}\text{Ti}_{1-x}\text{Zr}_x\text{O}_3$ is ascribed [8] to the dual substitution on the A and B sites. Detailed investigations of the possible segregation of the two substituted cations at nanoscale and thermodynamic properties are desirable to clear up the microscopic origin of the transition sequence observed.

The main purpose of the present paper is to reveal the heat capacity $C_p(T)$ and the thermal expansion $\alpha(T)$ behaviour of $\text{Ba}_{0.9}\text{Bi}_{0.067}\text{Ti}_{1-x}\text{Zr}_x\text{O}_3$ compounds over a wide temperature region and in the vicinity of T_c , T'_m and T''_m temperatures.

2. Experimental details

The compositions of the $\text{Ba}_{0.9}\text{Bi}_{0.067}(\text{Ti}_{1-x}\text{Zr}_x)\text{O}_3$ system were obtained from BaCO_3 , Bi_2O_3 , TiO_2 and ZrO_2 using the reaction [8]



Before the two heat treatments, 1 h grinding was carried out and powders were pressed under 100 MPa into 8 mm diameter discs about 5 mm thick. Calcination at 1200 °C for 15 h was followed by 4 h sintering at 1400 °C under an oxygen atmosphere.

Room temperature powder x-ray diffraction patterns were recorded on a Philips diffractometer using $\text{Cu K}\alpha$ radiation ($\lambda = 1.5406 \text{ \AA}$) in the angular range $5^\circ \leq 2\theta \leq 80^\circ$. This made it possible to verify that the samples were single phase and of perovskite type. This allows us to determine the limits of the solid solutions. The single phase corresponds to $0 \leq x \leq 1$.

The diameter shrinkage $(\Phi_{\text{init}} - \Phi_{\text{final}})/\Phi_{\text{init}}$ and the compactness (experimental density/theoretical density) were systematically determined. Their values were in the ranges 0.15–0.17 and 0.92–0.96, respectively.

Measurements of the heat capacity in a temperature range 100–420 K were carried out using a homemade automated adiabatic calorimeter [9], permitting us to obtain the absolute value of the heat capacity with a high accuracy. The sample mass was 3.80 g for $x = 0.04$ and 5.13 g for $x = 0.15$. Measurements were made using both the traditional discrete heating ($\Delta T = 1.0\text{--}2.5 \text{ K}$) and continuous heating at a temperature variation rate of about $dT/dt \approx (0.1\text{--}0.3) \text{ K min}^{-1}$. The accuracy of the measurements depends on the heating regime and amounts to (0.1–0.3)%.

Thermal expansion measurements were performed on the same ceramic samples using a quartz optical–mechanical dilatometer with a sensitivity of $1.2 \times 10^{-6} \text{ cm}$.

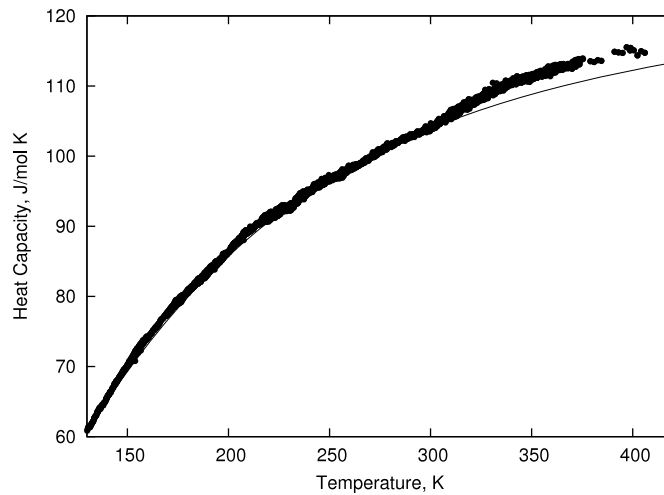


Figure 1. Heat capacity of $\text{Ba}_{0.90}\text{Bi}_{0.067}\text{Ti}_{1-x}\text{Zr}_x\text{O}_3$, $x = 0.04$. The solid line is the lattice specific heat.

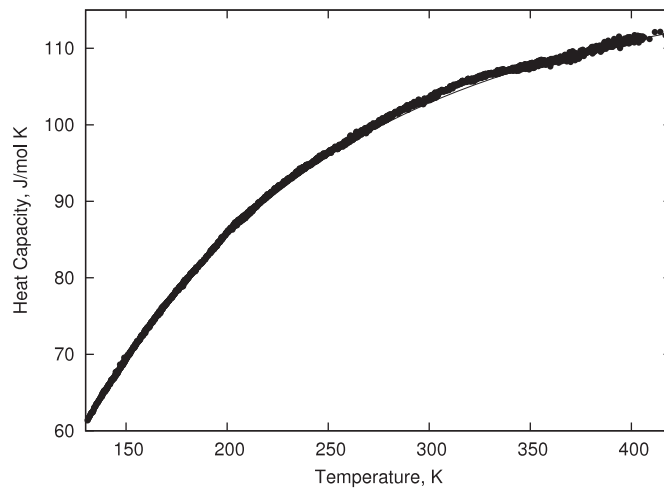


Figure 2. Heat capacity of $\text{Ba}_{0.90}\text{Bi}_{0.067}\text{Ti}_{1-x}\text{Zr}_x\text{O}_3$, $x = 0.15$. The solid line is the lattice specific heat.

3. Results and discussion

3.1. Heat capacity

The results of $\text{Ba}_{0.9}\text{Bi}_{0.067}(\text{Ti}_{0.96}\text{Zr}_{0.04})\text{O}_3$ (BBTZ4) ceramic heat capacity measurements are represented in figure 1. The curve describing the temperature dependence of the heat capacity does not exhibit clearly manifested anomalies typical for ordinary phase transitions. However, in the temperature regions 150–250 K and 300–400 K broad blurred anomalies in $C_p(T)$ are observed. A similar situation is observed for $\text{Ba}_{0.9}\text{Bi}_{0.067}(\text{Ti}_{0.85}\text{Zr}_{0.15})\text{O}_3$ (BBTZ15) ceramic (figure 2); however in the latter case heat capacity anomalies are displaced to temperature regions 200–250 K and 250–350 K.

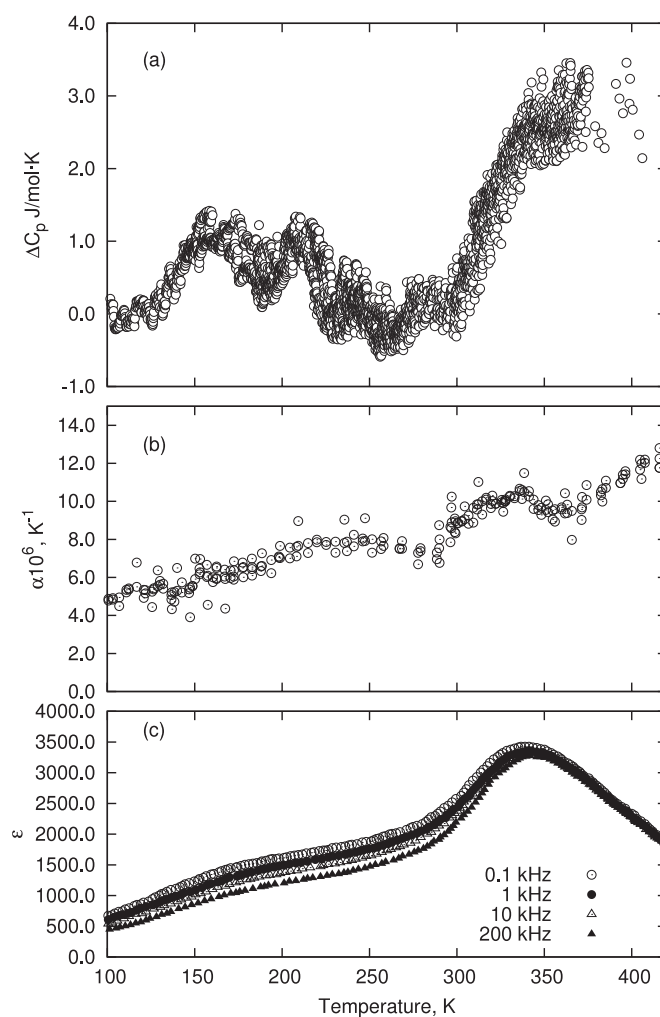


Figure 3. $\text{Ba}_{0.90}\text{Bi}_{0.067}\text{Ti}_{1-x}\text{Zr}_x\text{O}_3$, $x = 0.04$. Temperature dependences of the anomalous heat capacity (a), thermal expansion (b) and permittivity [8] (c).

To analyse these features in more detail the anomalous ΔC_p and lattice C_L contributions to the total heat capacity should be separated. This procedure was carried out using a simple model describing the lattice heat capacity of the compound as a combination of the Debye and Einstein functions. In the temperature range 100–420 K the heat capacity of the samples under investigation is already poorly sensitive to fine details of a vibration spectrum and the approximation of the lattice contribution carried out by this way is quite justified.

The heat capacity anomalies $\Delta C_p = C_p - C_L$ for both compounds under investigation reach only $\sim 1\text{--}3 \text{ J mol}^{-1} \text{ K}^{-1}$ or $\sim 1\text{--}3\%$ of C_L (figures 3(a) and 4(a)). However one can see clearly two features in the behaviour of ΔC_p concentrated near 180 and 370 K for BBTZ4 and near 230 and 330 K for BBTZ15. Unfortunately, the anomalous heat capacity components are fairly small, with the associated uncertainties reaching as high as 20–30%, which precluded any attempt at quantitative treatment.

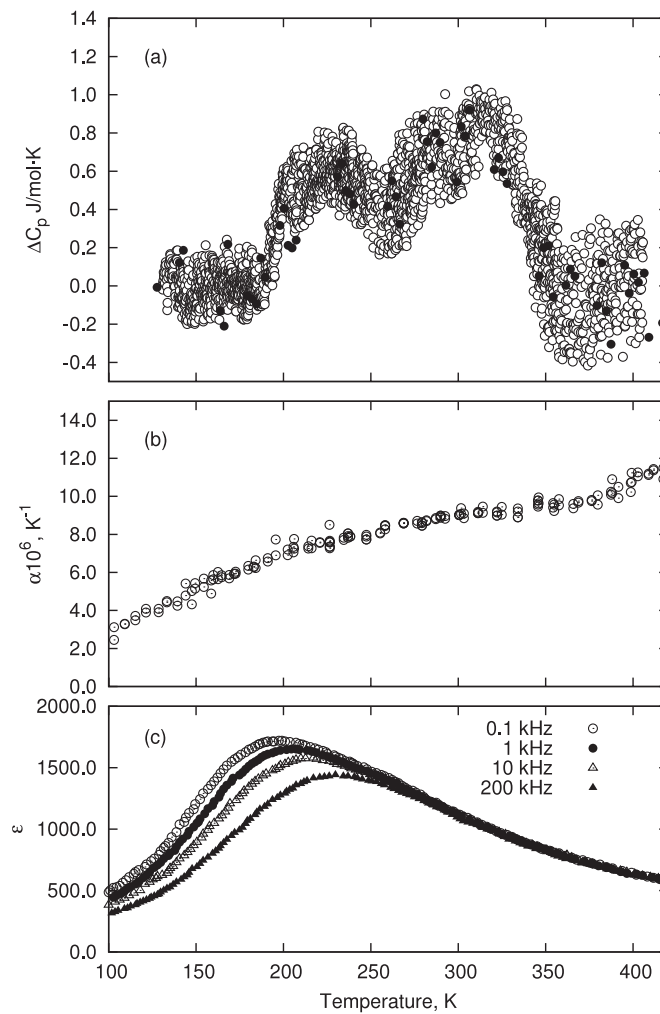


Figure 4. $\text{Ba}_{0.90}\text{Bi}_{0.067}\text{Ti}_{1-x}\text{Zr}_x\text{O}_3$, $x = 0.15$. Temperature dependences of the anomalous heat capacity (a), thermal expansion (b) and permittivity [8] (c).

The entropy change associated with the anomalous behaviour of the heat capacity is small ($\Delta S \sim 0.1\text{--}0.2R$) and demonstrates clearly the displacive nature of crystal phase changes. It should be noted that for barium-containing perovskites the heat capacity anomalies and the entropy changes are much less [10] than those for lead-containing relaxors such as PMN. In the latter the positional ordering of Pb ions is responsible for the main part of the entropy [11].

3.2. Thermal expansion

The results of the thermal expansion study on BBTZ4 and BBTZ15 are presented in figures 3(b) and 4(b). The linear thermal expansion coefficient $\alpha(T)$ of BBTZ15 shows, like the heat capacity, a smeared anomaly at about 350–370 K and a noticeable decrease at $T < 200$ K (figure 4(b)). For BBTZ4 there are two marked anomalies of $\alpha(T)$ at ~ 280 K and ~ 370 K and a pronounced change in the slope below 200 K (figure 3(b)).

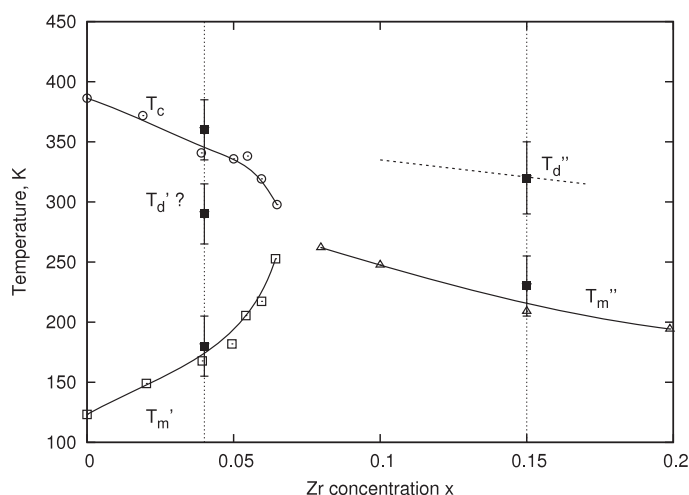


Figure 5. T - x phase diagram of $\text{Ba}_{0.90}\text{Bi}_{0.067}\text{Ti}_{1-x}\text{Zr}_x\text{O}_3$. Open circles, triangles and squares—dielectric data [8]; black squares with error bars—heat capacity and thermal expansion data.

3.3. T - x phase diagram

Figures 3 and 4 combine $\Delta C_p(T)$, $\alpha(T)$ and $\varepsilon(T)$ [8] to compare their anomalous behaviour. For BBTZ15 the situation is very similar to that for the $\text{BaTi}_{1-x}\text{Zr}_x\text{O}_3$ ($x > 0.3$) system with the usual sequence of phenomena observed [3, 6, 5, 4].

The heterovalent substitution of the Ba^{2+} cation with the Bi^{3+} one in $\text{BaTi}_{1-x}\text{Zr}_x\text{O}_3$ compounds introduces additional disorder on the A sites of the perovskite lattice. To compensate for the charge imbalance, vacancies on this site are introduced at the level of one vacancy for two Bi^{3+} substitutions, leading to the chemical formula $\text{Ba}_{1-y}\text{Bi}_{2y/3}\square_{y/3}\text{Ti}_{1-x}\text{Zr}_x\text{O}_3$. Bi^{3+} ions and cation vacancies can form defect clusters. A similar situation was observed and simulated for Nb^{5+} modified BaTiO_3 , where relaxor behaviour takes place at Nb concentrations of more than 6% [12, 13]. At high values of the Bi concentration in $\text{Ba}_{1-y}\text{Bi}_{2y/3}\square_{y/3}\text{Ti}_{1-x}\text{Zr}_x\text{O}_3$ ($2y/3 = 0.067$) long-range ferroelectric order can be broken down by defect clustering, but local polar order is preserved within defect-free regions giving rise to the $\varepsilon(T)$ anomaly at T_m'' .

So we associate the first anomaly of the BBTZ15 heat capacity in the temperature range 250–370 K with polar nanoregion formation near the Burns temperature T_d'' (approximately the temperature at which the deviation of $1/\varepsilon(T)$ from the Curie–Weiss law was observed [8]) and the second one in the range 150–250 K, which coincides with the region of anomalous behaviour of the permittivity [8], with polar nanoregion interaction near T_m'' (figure 4).

For BBTZ4 we observe C_p anomalies near 120–250 K and in the temperature interval 300–400 K (figure 3(a)). The high temperature anomaly coincides with the anomaly of $\varepsilon(T)$ at T_c and corresponds to the paraelectric to ferroelectric phase transition. The low temperature anomaly is observed near T_m' which is the relaxor temperature. However, there is no clear indication of a specific heat anomaly at the related Burns temperature, probably because of its proximity to T_c , the ferroelectric phase transition. The nature of the anomaly in $\alpha(T)$ near 250–300 K is undecided (figure 3(b)) but we still can ascribe it to the Burns temperature T_d' of BBTZ4 (figure 5). This will be confirmed in the next part which deals with a computation of the root mean square polarization from the thermal expansion data.

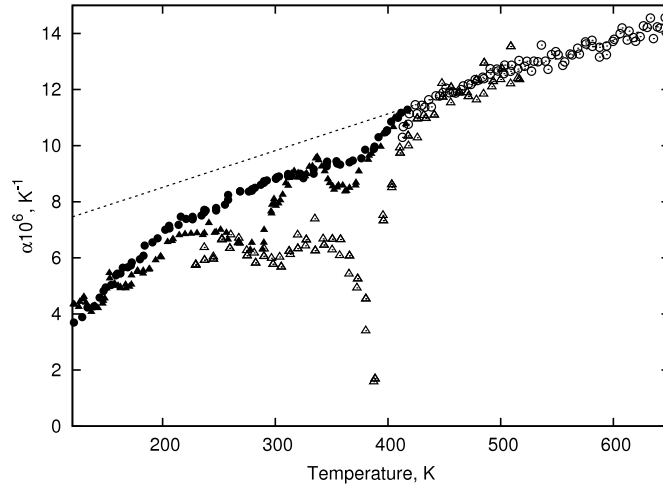


Figure 6. Thermal expansion coefficient for $\text{Ba}_{0.90}\text{Bi}_{0.067}\text{Ti}_{1-x}\text{Zr}_x\text{O}_3$ (\blacktriangle — $x = 0.04$, \bullet — $x = 0.15$) and BaTiO_3 (\circ —[14], \triangle —[15]). The dashed line represents the fitting of data [14] taken at $T > 450$ K.

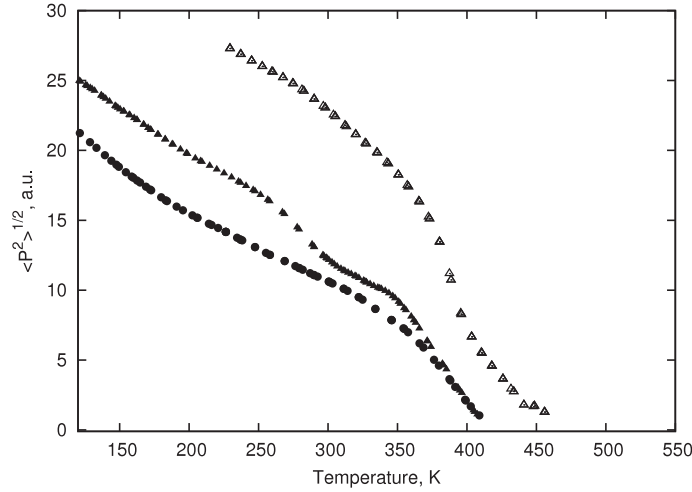


Figure 7. Temperature dependences of the rms polarization for $\text{Ba}_{0.90}\text{Bi}_{0.067}\text{Ti}_{1-x}\text{Zr}_x\text{O}_3$ (\blacktriangle — $x = 0.04$, \bullet — $x = 0.15$) and BaTiO_3 (\triangle) [15].

3.4. Root mean square polarization

For ferroelectric relaxors even though $\langle P \rangle = 0$ we have $\langle P^2 \rangle \neq 0$ and there is an additional contribution to the strain proportional to $\langle P^2 \rangle$, due to electrostriction. This contribution vanishes only above the Burns temperature T_d where $\langle P^2 \rangle = 0$. So one can estimate the temperature dependences of the strain and the root mean square polarization $\langle P^2 \rangle^{1/2}$ from thermal expansion data, presented above.

The thermal expansion coefficients $\alpha(T)$ for two $\text{Ba}_{0.90}\text{Bi}_{0.067}(\text{Ti}_{1-x}\text{Zr}_x)\text{O}_3$ compounds and for pure BaTiO_3 [14, 15] are shown in figure 6. At high temperatures, $\alpha(T)$ shows a

nearly linear temperature dependence in BaTiO₃ [14]. Upon further cooling the temperature dependence changes in BaTiO₃ and $\alpha(T)$ starts to decrease more steeply. The anomaly is connected with the ferroelectric phase transition at $T_c \approx 400$ K.

The strain contribution due to polarization can be expressed as

$$\Delta s(T) = s(T) - s_r(T) = \int (\alpha(T) - \alpha_r(T)) dT = (Q_{11} + 2Q_{12}) \langle P^2 \rangle,$$

where $\alpha_r(T)$ is the regular contribution to the thermal expansion coefficient, fitted by a linear function for BaTiO₃ data [14] at $T > 450$ K. Results of the $\langle P^2 \rangle^{1/2}$ calculations are shown for Ba_{0.90}Bi_{0.067}Ti_{1-x}Zr_xO₃ and BaTiO₃ [15] in figure 7.

4. Conclusion

Two compositions of solid solutions Ba_{0.90}Bi_{0.067}Ti_{1-x}Zr_xO₃ ($x = 0.04$ and 0.15) characterized by different conditions of the relaxor state appearance have been studied by calorimetric and dilatometric methods. The thermal property anomalies were found at all special temperatures inherent to relaxors. The temperature behaviour of the root mean square polarization of the solid solutions studied is compared with the data for BaTiO₃.

Acknowledgments

This work was supported by the Russian Foundation for Basic Research (project no. 07-02-00069) and the Council on Grants from the President of the Russian Federation for Support of Leading Scientific Schools (project no. NSh-4137.2006.2).

References

- [1] Ravez J and Simon A 1997 *Eur. J. Solid State Inorg. Chem.* **34** 1199
- [2] Farhi R, Marssi M El, Simon A and Ravez J 1999 *Eur. Phys. J. B* **9** 599
- [3] Simon A, Ravez J and Maglione M 2004 *J. Phys.: Condens. Matter* **16** 963
- [4] Bokov A A, Maglione M and Ye Z-G 2006 *J. Phys.: Condens. Matter* **19** 092001
- [5] Bokov A A, Maglione M, Simon A and Ye Z-G 2006 *Ferroelectrics* **337** 169
- [6] Gorev M, Bondarev V, Sciau Ph and Savariault J-M 2006 *J. Phys.: Condens. Matter* **18** 4407
- [7] Ravez J and Simon A 2001 *J. Solid State Chem.* **162** 260
- [8] Simon A, Ravez J and Maglione M 2005 *Solid State Sci.* **7** 925
- [9] Gorev M V, Gekk P I, Iskornev I M, Kot L A, Gonyaev V S, Flerov I N and Cherepanov V A 1988 *Izmer. Tekh.* **8** 33
- [10] Gorev M V, Flerov I N, Bondarev V S, Sciau Ph and Savariault J-M 2004 *J. Phys.: Condens. Matter* **16** 7143
- [11] Gorev M V, Flerov I N, Bondarev V S and Sciau Ph 2003 *JETP* **96** 531
- [12] Simon A and Ravez J 2003 *Solid State Sci.* **5** 1459
- [13] Zhang R, Li J F and Viehland D 2004 *Comput. Mater. Sci.* **29** 67
- [14] Mueller V, Jäger L, Beige H, Abricht H-P and Müller T 2004 *Solid State Commun.* **129** 757
- [15] He Y 2004 *Thermochim. Acta* **419** 135